STATISTICS, OPTIMIZATION AND INFORMATION COMPUTING
Stat., Optim. Inf. Comput., Vol. **14**, September 2025, pp 0–16.
Published online in International Academic Press (www.IAPress.org)

A Modified Monsef Distribution Using Quadratic Rank Transformation Map

M.M.E. Abd El-Monsef*, T.A. Alghazi, H.H. El-Damrawy

Faculty of Science, Tanta University, Egypt

Abstract A new distribution is proposed using the Quadratic Rank Transmutation Map (QRTM), which introduces skew to an initial symmetric base distribution. The Monsef distribution serves as the baseline. Various statistical properties, including moments, the moment-generating function, and the characteristic function, are derived. The parameters are estimated using the maximum likelihood estimation method, and the method's performance is validated through mean squared errors and average biases. Additionally, two real datasets are used to demonstrate the flexibility of the proposed distribution.

Keywords Quadratic rank transformation map; Monsef distribution; The Maximum likelihood estimation.

DOI: 10.19139/soic-2310-5070-2344

1. Introduction

In modern decades proposing new probability distributions became a common enactment. Many researchers are interested in proposing new probability distributions by attaching an extra parameter to the baseline distribution. Some researchers are interested in using transformations whereas others introduce new probability distributions by using generators or by combining two or more distributions. Over the last few years researchers have extensive desires for the pertinence of inverse transformations of probability distributions and their applications. Modeling the real-life data is the foremost purpose of such amendment. What differentiates the new distributions with the existing probability distributions is the increase in model flexibility for modeling complex data structures. Probability distributions are broadly using in different areas including biomedical, environmental studies, economics, engineering and reliability. The development of new methods of expanding the existing distributions is quite rich in the literature of distribution theory. There are several methods to propose new distributions by the use of some baseline distribution in statistical literature. This has been done through different approaches. The most popular among them is the power transformation initiated by Gupta et al. (1998). The transformation based on the generalization of Kumar et al. (2015) called Generalized DUS (GDUS) transformation proposed by Maurya et al. (2017). The DUS transformation—named after its developers, Dinesh, Umesh, and Sanjay (Maurya et al., 2016)—is a statistical technique that modifies baseline distributions through exponential adjustments to the cumulative distribution function (CDF), improving their adaptability for real-world data. Kyurkchiev (2017) developed a transformation method to create sigmoid functions based on the Logistic distribution. Statisticians have particularly focused on transformation maps like the sample transformation map (STM) $y = G^{-1}[F(x)]$ and rank transformation map $v = G[F^{-1}(u)]$.

Apart from the above, in many applied areas like lifetime analysis and insurance analysis we need extended distributions, that is, new distributions which are more flexible to model real data, since the data can present a high degree of skewness and kurtosis. Thus, we suggested more flexible distributions by adding a parameter to existing distribution to generate transmuted distribution. Which is the quadratic rank transmutation map (QRTM)

*Correspondence to: M.M.E. Abd El-Monsef (Email: mmezzat@science.tanta.edu.eg). Faculty of Science, Tanta University, Egypt.

ISSN 2310-5070 (online) ISSN 2311-004X (print)

proposed by Shaw and Buckley (2007). An application of the quadratic rank transmutation is extended to the Monsef distribution. The distributional characteristics of the generated transmuted distributions are also simulated to compare with traditional Monsef distribution. The distributional characteristics of the generated transmuted distributions are also simulated to compare with traditional Monsef distribution. Using this transformation many distributions have been derived. By this, there is also an overview of most studied used on the modifications of the QRTM. For example, Abd El Hady (2014), proposed a new Weibull distribution by using exponentiated QRTM. Alizadeh et al. (2015) studied generated a new distribution family by considering exponentiated distribution as a baseline distribution. Merovci (2013), introduced a new distribution by taking a baseline distribution as exponentiated exponential distribution.

Eltehiwy and Ashour (2013) introduced transmuted exponentiated modified Weibull distribution, and Ashour and Eltehiwy (2013) introduced transmuted exponentiated Lomax distribution. These last three studies can be seen as a special case of Alizadeh et al. (2015). Mansour et al. (2015) proposed new transmutation map by adding two extra parameters to get more flexible distribution. Then, Mansour and Mohamed (2015) introduced a new Lindley distribution by using this new transmutation map approach. Das and Barman (2015) introduced a kind of generalization of QRTM by considering sum of k- dimensional vector of transmutation parameters. There are two similar studies that respectively are the generalized transmuted G family by Nofal et al. (2017) and generalized transmuted Weibull distribution by Nofal and El Gebaly (2017). Recently in (2022) Onyekwere et al. proposed a modification of Shanker distribution using the quadratic rank transmutation map.

Researchers are actively building on the DUS (Dinesh-Umesh-Sanjay) transformation, creating more powerful versions to model complex data. For instance, Gauthami and Chacko (2024) and Thomas and Chacko (2023) developed a "Power Generalized" variant, while Mohammed, Hassan, and Yahaya (2024) created an entire new family of distributions based on the DUS-Topp-Leone framework. These new models are being applied to classic distributions like the Inverse Kumaraswamy (Gauthami and Chacko, 2024), Inverse Rayleigh (Khan and Mustafa, 2023), Weibull, and Lomax (Thomas and Chacko, 2023) to give them more flexibility. The real-world value of these models is proven through applications in areas like reliability engineering (Gauthami and Chacko, 2024) and other engineering data fits (Unnikrishnan, Chacko, and Thomas, 2023). The field is even expanding to handle uncertain data, as Megha, Divya, and Sajesh (2025) introduced a neutrosophic version of the DUS transformation for imprecise datasets.

According to the Quadratic Rank Transmutation Map (QRTM); a random variable X is said to have a transmuted distribution if its cumulative distribution function CDF is given by

$$G(x) = (1+\lambda)F(x) - \lambda F^2(x); \quad |\lambda| \leq 1$$

where $F(x)$ is the CDF of the original distribution and $G(x)$ is the CDF of the generated distribution. The absolute value of λ should be kept below one, as increasing it beyond one result in the function yielding negative values, which is, of course, unacceptable. Observe that at $\lambda = 0$ we have the base distribution. The benefit of using this map is that its inverse is available in closed form as follows:

$$G^{-1}(u) = F^{-1}\left(\frac{1+\lambda-\sqrt{(1+\lambda)^2-4\lambda u}}{2\lambda}\right)$$

Consequently, QRTM introduces skewness to a symmetric base distribution, although there is no strict requirement for the base distribution $F(x)$ to be symmetric. If $F(x)$ is symmetric about the origin, then the distribution of the square of the transmuted random variable will match the distribution of the square of the original random variable.

The QRTM outperforms alternative transformation methods like the Exponentiated QRTM (EQRTM) and Generalized DUS (GDUS) due to its balanced flexibility and simplicity. Unlike EQRTM, which only stretches tails monotonically via a power parameter $F(x)^k$, QRTM's additive skewness term $\lambda F(x)^2$ allows bidirectional skewness control $\lambda \in [-1, 1]$, making it adaptable to both left- and right-skewed data. Compared to GDUS, which relies on exponential transformations $\frac{e^{F(x)}-1}{e-1}$, QRTM preserves closed-form quantiles and interpretable parameters

without overparameterization. Thus, QRTM strikes an optimal trade-off between flexibility, interpretability, and robustness.

The paper is organized as follows. Constructing the PDF of quadratic rank transformation map Monsef distribution (QRTMD) in section 2. In section 3, some statistical properties and reliability measures of the QRTMD are obtained. We introduced the maximum likelihood estimation for the unknown parameters in section 4. In section 5, Simulation study has been conducted for various sample sizes and parameter values. We examine the flexibility of our model by using two real datasets applications in section 6.

2. Quadratic Rank Transformation Map Monsef Distribution

Monsef distribution is a flexible baseline as its PDF combines polynomial and exponential terms, allowing it to model right-skewed, non-negative data (e.g., lifetime, financial, or environmental data). Its CDF is analytically tractable, facilitating derivations of QRTMD's properties (e.g., moments, hazard functions). Moreover, the scale parameter θ controls dispersion, making it suitable for data with varying spread.

While the Monsef distribution offers a tractable baseline for non-negative data, its limited flexibility in skewness and tail behavior motivates the use of QRTM. By transmuting Monsef distribution's CDF via QRTM, we introduce a skewness parameter λ that enhances shape versatility without sacrificing closed-form expressions for statistical properties. The proposed quadratic rank transformation map Monsef distribution (QRTMD) can be attained as follows:

Let the baseline distribution be Monsef distribution (MD) with,

$$f(x) = \frac{\theta^3}{2+\theta(2+\theta)}(x+1)^2 e^{-x\theta}; \quad 0 < x < \infty.$$

where the CDF of MD is

$$F(x) = \frac{2+\theta(2+\theta)+e^{-x\theta}\left(-2-(1+x)\theta(2+\theta+x\theta)\right)}{2+\theta(2+\theta)}, \quad \theta > 0.$$

Using the following quadratic rank transformation map:

$$G(x) = (1+\lambda)F(x) - \lambda F^2(x); \quad |\lambda| \leq 1,$$

where $F(x)$ is the CDF of the MD and $G(x)$ is the CDF of the QRTMD.
Then the CDF of the QRTMD can be written as:

$$G(x) = 1 - \frac{1}{\left(2+\theta(2+\theta)\right)^2} e^{-2x\theta}\left(2+(1+x)\theta(2+\theta+x\theta)\right) \left(-e^{x\theta}\left(2+\theta(2+\theta)\right)(-1+\lambda) + \left(2+(1+x)\theta(2+\theta+x\theta)\right)\lambda\right); \quad x, \theta > 0; |\lambda| < 1. \quad (1)$$

and the PDF of the QRTMD is given by

$$g(x) = \frac{e^{-2x\theta}(1+x)^2\theta^3\left(-e^{x\theta}\left(2+2\theta+\theta^2\right)(-1+\lambda)+2\left(2+2(1+x)\theta+(1+x)^2\theta^2\right)\lambda\right)}{\left(2+2\theta+\theta^2\right)^2}, \quad x, \theta > 0; |\lambda| < 1. \quad (2)$$

The parameter θ scales the probability distribution; if the value of the scale parameter is large then distribution is more spread out or more stretching and if the value is small then distribution will be concentrated or compressed.

On the other hand, the parameter λ affects the general shape of the PDF. It's responsible for changing the skewness and kurtosis of the distribution. The PDF of the QRTMD can be unimodal or decreasing as shown in Figure 1. The PDF of the QRTMD tends to $\frac{\theta^3(1+\lambda)}{2+\theta(2+\theta)}$ when $x \to 0$ and tends to zero when $x \to \infty$.

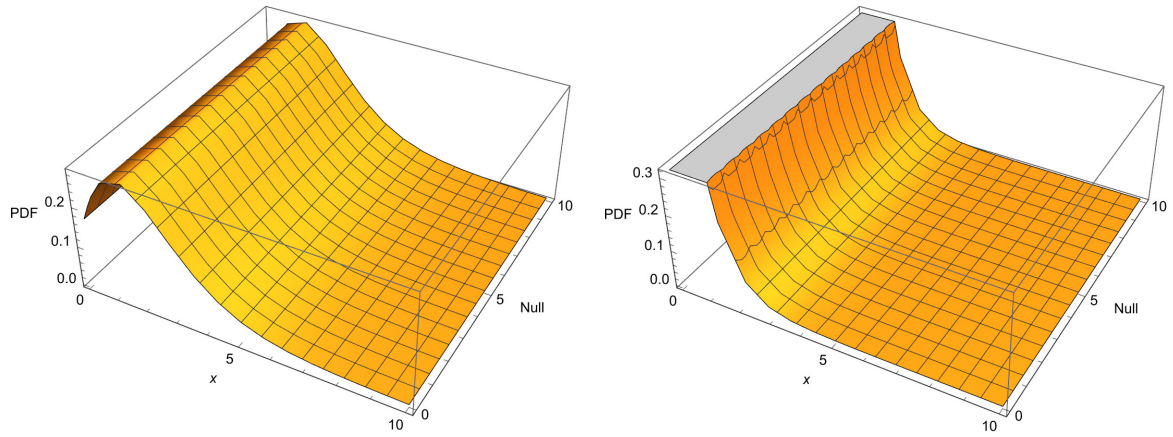

$\lambda = 0.9; \theta = 0.7$ $\lambda = 0.7; \theta = 1.7$

Figure 1. PDF behavior of the QRTMD

In addition to the many applications of decreasing probability functions, the skewed unimodal PDFs are useful in modeling stock returns, which are often asymmetrical due to investor biases and reactions to news. In economics, income distribution is typically skewed and can be represented by a skewed unimodal PDF to model wealth or income inequality. In environmental monitoring, skewed unimodal PDFs can model data like air pollutant concentration levels which are often skewed, with a peak at lower levels and a tail that represents rare high-pollution events. It also can model the distribution of disease cases, especially when outbreaks have a sharp peak that diminishes over time or varies by demographic.

3. Statistical Properties

Some statistical properties of the QRTMD will be summarized.

3.1. Moments

If the random variable X has the QRTMD, then the r^{th} moment can be written as

$$\begin{aligned}\mu'_r = \int_0^\infty x^r g(x)dx = -\frac{1}{(2+2\theta+\theta^2)^2}2^{-4-r}\theta^{-r}(-r^4\lambda - 2r^3(7+4\theta)\lambda \\ + 16\left(2+2\theta+\theta^2\right)^2(-2^r + (-1+2^r)\lambda) + r^2(-2^{5+r} + (-67+2^{5+r})\lambda \\ + 8\theta^2(-2^{1+r} + (-3+2^{1+r})\lambda) + 8\theta(-2^{2+r} + (-9+2^{2+r})\lambda)) \\ + 2r(-32^{4+r} + (-59+32^{4+r})\lambda + 16\theta^3(-2^r + (-1+2^r)\lambda) \\ + 16\theta(-52^r + (-6+52^r)\lambda) + \theta^2(-72^{3+r} + (-60+72^{3+r})\lambda)))(1+r). \quad (3)\end{aligned}$$

From (2) the first and second moments of the QRTMD are,

$$\mu = \frac{4\left(2+\theta(2+\theta)\right)\left(6+\theta(4+\theta)\right) - \left(15+2\theta\left(15+\theta\left(15+\theta(6+\theta)\right)\right)\right)\lambda}{4\theta\left(2+\theta(2+\theta)\right)^2} \tag{4}$$

$$\mu_2' = \frac{8\left(2+\theta(2+\theta)\right)\left(12+\theta(6+\theta)\right) - 3\left(35+2\theta(3+\theta)\left(10+\theta(5+\theta)\right)\right)\lambda}{4\theta^2\left(2+\theta(2+\theta)\right)^2} \tag{5}$$

Respectively, the variance will be,

$$\begin{aligned}\mu_2 = -\frac{1}{16\theta^2\left(2+2\theta+\theta^2\right)^4}\Big(&-4\left(2+2\theta+\theta^2\right)^2\left(8\left(2+\theta(2+\theta)\right)\left(12+\theta(6+\theta)\right)\right.\\ &-3\left(35+2\theta(3+\theta)\left(10+\theta(5+\theta)\right)\right)\lambda) + \left(-4\left(2+\theta(2+\theta)\right)\left(6+\theta(4+\theta)\right)\right.\\ &\left.\left.+\left(15+2\theta\left(15+\theta\left(15+\theta(6+\theta)\right)\right)\right)\lambda\right)^2\Big)\end{aligned} \tag{6}$$

Similarly, the 3^{rd} and 4^{th} moments about the means can be derived as in the Appendix (A.1 and A.2).

3.2. The Skewness and Kurtosis

The skewness of a distribution β_1 is defined as the lack of symmetry, while kurtosis β_2 is a measure of how fat the tail is of any probability distribution. β_1 and β_2 are given in the Appendix (A.3 and A.4).

3.3. The Coefficient of Variation

The coefficient of variation CoV is the ratio between the standard deviation and the average and it's used to compare the variation between datasets.

$$\begin{aligned}CoV = &\frac{1}{\left(4\left(2+\theta(2+\theta)\right)\left(6+\theta(4+\theta)\right) - \left(15+2\theta\left(15+\theta\left(15+\theta(6+\theta)\right)\right)\right)\lambda\right)}\\ &\times\Big(\left(16(2+\theta(2+\theta))^2(12+\theta(2+\theta)(12+\theta(6+\theta))) - 4(2+\theta(2+\theta))\right.\\ &\left.(30+\theta(90+\theta(135+2\theta(66+\theta(39+\theta(10+\theta))))))\lambda - (15+2\theta(15+\theta(15+\theta(6+\theta))))^2\lambda^2\Big)^{1/2}\end{aligned} \tag{7}$$

3.4. The Moment Generating Function (MGF) and the Characteristic Function (CHF)

If the random variable X has the QRTMD, then the MGF and the CHF of X, denoted by $M_X(t)$ and $\phi_x(t)$ are derived as in the Appendix (A.5 and A.6).

3.5. Some Reliability Measures

The survival function is a statistical measure represents the probability of an individual not experiencing an event before a certain time. Thus, the survival function of the QRTMD is given by

$$\begin{aligned}&S(x) = \frac{e^{-2x\theta}B(x,\theta)}{A(\theta)^2} \times \Psi(x,\theta,\lambda)\\ &\text{where}\\ &\Psi(x,\theta,\lambda) = -e^{x\theta}A(\theta)(\lambda-1) + B(x,\theta)\lambda\\ &A(\theta) = 2+\theta(2+\theta)\\ &B(x,\theta) = 2+(1+x)\theta(2+\theta+x\theta)\end{aligned} \tag{8}$$

The hazard function is defined as the rate of failure of the system, on condition that the failure has not occurred before to time. Thus, the hazard function of the QRTMD is

$$H(x) = \frac{(1+x)^2\theta^3\left(-e^{x\theta}\left(2+\theta(2+\theta)\right)(-1+\lambda)+2\left(2+(1+x)\theta(2+\theta+x\theta)\right)\lambda\right)}{\left(2+(1+x)\theta(2+\theta+x\theta)\right)\left(-e^{x\theta}\left(2+\theta(2+\theta)\right)(-1+\lambda)+\left(2+(1+x)\theta(2+\theta+x\theta)\right)\lambda\right)} \tag{9}$$

The hazard function of the QRTMD exhibits flexible shape behavior as shown in Figure 2, capable of assuming increasing and increasing-decreasing-increasing forms, making it suitable for modeling diverse failure patterns.

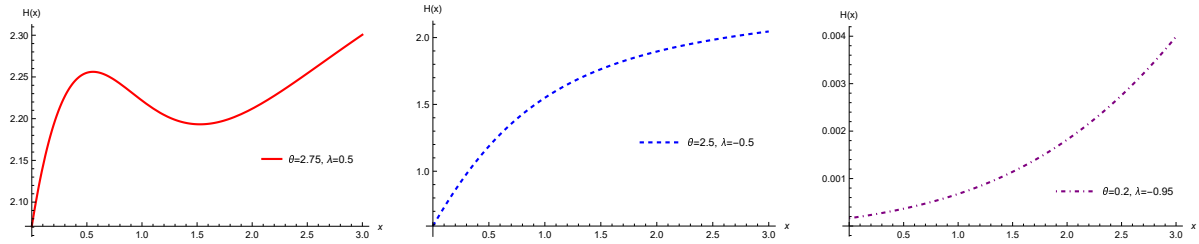

Figure 2. Hazard function behavior of the QRTMD

The Mills Ratio, presented by Mills 1926, is the reciprocal of the hazard function. The inverse of the Mills ratio used commonly in regression analysis for detecting the potential selection bias. For the QRTMD, the Mills ratio is

$$\begin{aligned}
&\text{Mills}(x,\theta,\lambda) = \frac{1}{(1+x)^2\theta^3} \times \frac{B(x,\theta)}{\Psi(x,\theta,\lambda)} \times \Psi(x,\theta,\lambda) \\
&\text{where} \\
&\Psi(x,\theta,\lambda) = -e^{x\theta}A(\theta)(\lambda-1) + B(x,\theta)\lambda \\
&A(\theta) = 2+\theta(2+\theta) \\
&B(x,\theta) = 2+(1+x)\theta(2+\theta+x\theta)
\end{aligned} \tag{10}$$

The analysis and graphical representation of income inequality are frequently conducted using Bonferroni and Lorenz curves. The Lorenz curve, $L(p)$, represents the proportion of the total income volume that entities with income equal to or less than volume an accumulate. The Bonferroni curve, $B(p)$, is the scaled conditional mean curve, calculated as the ratio of the mean income of a group to the total income volume of the population. Lorenz and Bonferroni curves derived below and illustrated in Figure 3.

$$L(x) = \frac{1}{4A(\theta)C(\theta)-D(\theta)\lambda} \times \begin{pmatrix} 4A(\theta)C(\theta)-D(\theta)\lambda \\ +4e^{-x\theta}A(\theta)\Big(C(\theta)+x\big(6+\theta(4+3x+(1+x)^2\theta)\big)\Big)(\lambda-1) \\ -e^{-2x\theta}\Big(33+2\theta\big(25+33x+(1+x)(17+33x)\theta \\ +2(1+x)^2(3+11x)\theta^2+(1+x)^3(1+9x)\theta^3 \\ +2x(1+x)^4\theta^4\big)\Big)\lambda \end{pmatrix} \tag{11}$$

where

$$\begin{aligned}
A(\theta) &= 2+\theta(2+\theta) \\
C(\theta) &= 6+\theta(4+\theta) \\
D(\theta) &= 15+2\theta(15+\theta(15+\theta(6+\theta)))
\end{aligned}$$

For Bonferroni we have,

$$B(x) = \frac{1}{\Delta(\theta,\lambda)} \times \frac{1}{1-\Phi(x,\theta,\lambda)} \times N(x,\theta,\lambda)$$

where

$$\Delta(\theta,\lambda) = 4A(\theta)C(\theta) - D(\theta)\lambda$$

$$\Phi(x,\theta,\lambda) = \frac{1}{A(\theta)^2} e^{-2x\theta} B(x,\theta)\left(-e^{x\theta}A(\theta)(\lambda-1) + B(x,\theta)\lambda\right)$$

$$\begin{aligned} N(x,\theta,\lambda) &= 4A(\theta)C(\theta) + 4e^{-x\theta}A(\theta)\left(C(\theta) + x\left(6+\theta(4+3x+(1+x)^2\theta)\right)\right)(\lambda-1) \\ &\quad - e^{-2x\theta}\left(33 + 2\theta\left(25 + 33x + (1+x)(17+33x)\theta + 2(1+x)^2(3+11x)\theta^2\right.\right. \\ &\quad \left.\left. + (1+x)^3(1+9x)\theta^3 + 2x(1+x)^4\theta^4\right)\right)\lambda - D(\theta)\lambda \end{aligned} \tag{12}$$

and

$$A(\theta) = 2 + \theta(2+\theta)$$

$$B(x,\theta) = 2 + (1+x)\theta(2+\theta+x\theta)$$

$$C(\theta) = 6 + \theta(4+\theta)$$

$$D(\theta) = 15 + 2\theta(15 + \theta(15 + \theta(6+\theta)))$$

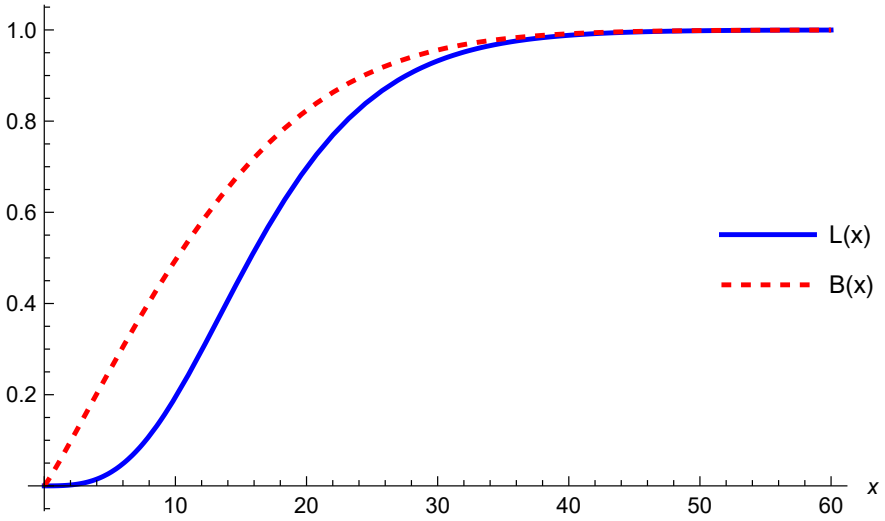

Figure 3. Bonferroni and Lorenz curves for the QRTMD at $\theta = 0.25; \lambda = -0.5$

The Gini index G (Gini 1914) is an inequality indicator computed using the Lorenz curve. The Gini index is the measurement of the ratio between the concentration area and its theoretical maximum. The $Gini\ Index$ of the QRTMD is given by

$$\begin{aligned} G = \frac{1}{\left(\theta\left(-4\left(2+\theta(2+\theta)\right)\left(6+\theta(4+\theta)\right) + \left(15+2\theta\left(15+\theta\left(15+\theta(6+\theta)\right)\right)\right)\lambda\right)\right.} \\ \times \left[1 - (2e^{-2\theta}(8e^{\theta}(2+\theta(2+\theta))(12+\theta(15+2\theta(4+\theta)))(-1+\lambda)\right. \\ - (87+\theta(249+4\theta(83+2\theta(33+4\theta(4+\theta)))))\lambda + e^{2\theta}(192 - 4\theta(-60-32\theta+4\theta^3+\theta^4) \\ \left.\left. + (-105+\theta(-165+2\theta(-60+\theta(-9+\theta(3+\theta)))))\lambda)\right)\right] \end{aligned} \tag{13}$$

4. Maximum Likelihood Estimation

Let $x_i, i = 1, 2, 3, \ldots, n$ be a random from the QRTMD with parameters (θ, λ), then the log likelihood function is given by

$$L = 3n \ln \theta - 2n \ln \left(2 + 2\theta + \theta^2\right) - 2\theta \sum_{i=1}^{n} x_i + 2 \sum_{i=1}^{n} \ln \left(1 + x_i\right) + \sum_{i=1}^{n} \ln \left[(\lambda - 1) \left(2 + 2\theta + \theta^2\right) e^{-x_i \theta} + 2\lambda \left(2 + (1 + x_i)\, \theta \left(2 + \theta + x_i \theta\right)\right)\right]$$

For the parameters are obtained by taking their derivatives partially w.r.t its parameters, are as follows:

$$\begin{aligned} \frac{\partial\, L}{\partial \theta} =& \frac{3n}{\theta} - \frac{4n(1+\theta)}{A(\theta)} + 2 \sum_{i=1}^{n} x_i \\ &+ \sum_{i=1}^{n} \frac{1}{4\theta A(\theta)(-1+\lambda)\lambda(1+x_i)(2\theta+\theta x_i)} \times \\ &\Bigg(e^{\theta x_i} \Big(4e^{-\theta x_i} \theta A(\theta)(-1+\lambda)\lambda(1+x_i)(2+x_i) \\ &\quad + 4e^{-\theta x_i} \theta (2+2\theta)(-1+\lambda)\lambda(1+x_i)(2\theta+\theta x_i) \\ &\quad + 4e^{-\theta x_i} A(\theta)(-1+\lambda)\lambda(1+x_i)(2\theta+\theta x_i) \\ &\quad - 4e^{-\theta x_i} \theta A(\theta)(-1+\lambda)\lambda x_i (1+x_i)(2\theta+\theta x_i) \Big) \Bigg) \end{aligned} \tag{14}$$

where $A(\theta) = 2 + 2\theta + \theta^2$.

$$\frac{\partial\, L}{\partial \lambda} = \sum_{i=1}^{n} \frac{e^{-\theta x_i} A(\theta) + 2B(x_i, \theta)}{e^{-\theta x_i} A(\theta)(\lambda - 1) + 2\lambda B(x_i, \theta)} \tag{15}$$

where

$$\begin{aligned} A(\theta) &= 2 + 2\theta + \theta^2 \\ B(x_i, \theta) &= 2 + \theta(1 + x_i)(2 + \theta + \theta x_i) \end{aligned}$$

The ML estimators of the parameters θ and λ are obtained by solving the previous nonlinear system of equations. These equations can be solved iteratively till sufficiently close estimates of the parameters are obtained.

5. Simulation

Several methods were used for estimating the parameters of the QRTMD. Maximum Likelihood Estimation (MLE) is a premier technique that identifies the parameter values which make the observed data most probable. In contrast, the Method of Moments (MOM) offers a more intuitive strategy by matching theoretical moments of the distribution to their empirical sample equivalents. For regression-based models, the Ordinary Least Squares (LSE) method serves as a cornerstone, finding parameters that minimize the overall sum of squared errors between the model's predictions and the actual data. This approach is generalized by Weighted Least Squares (WLS), which introduces a weighting scheme to adjust for unequal variance across observations, thereby improving efficiency.

Lastly, the Cramér–von Mises (CVM) estimator belongs to the family of minimum distance estimators, which operates by minimizing the discrepancy between the empirical and theoretical cumulative distribution functions, providing a powerful goodness-of-fit criterion for estimation.

The QRTMD introduces two key parameters: the scale parameter θ which controls the spread and decay rate of the distribution and the skewness parameter λ which governs the direction and intensity of asymmetry. For large θ; the distribution decays rapidly, modeling data with shorter tails and for small θ; the PDF spreads out, capturing long-tailed processes. The parameter λ acts as a 'skewness switch': positive values ($\lambda > 0$) stretch the right tail to model rare high extremes (e.g., financial windfalls), while negative values ($\lambda < 0$) accentuate the left tail for frequent low-magnitude events (e.g., minor insurance claims). Meanwhile, θ scales the distribution's spread, with small values fitting long-tailed processes (e.g., catastrophe risks) and large values describing concentrated data (e.g., manufacturing tolerances). This dual interpretability makes QRTMD uniquely suited for fields like hydrology, finance, and reliability engineering. A simulation study has been conducted for various sample sizes and parameter values. The simulation study is repeated 1000 times each with sample size $n = 20, 40, 60, 80, 100, 500$ and 900 and parameter vectors $(\theta, \lambda) = (1.5, 0.5), (0.1, 1)$ and $(0.01, -1)$. The selection of these values reflects the two shapes of the pdf (decreasing and unimodal). This helps us to study the properties of the estimators in all pdf behaviours. The following algorithm was used for generating random samples from the QRTMD:

Algorithm

1. Generate $U_i \sim Uniform(0, 1); i = 1, 2, \ldots, n.$
2. Set $X_i = F^{-1}\left(\frac{1+\lambda-\sqrt{(1+\lambda)^2-4\lambda U_i}}{2\lambda}\right)$

The MLE, MOM, LSE, WLS and CVM simulation schemes for θ, λ were obtained via numerical optimization in Mathematica, enforcing $-1 \leq \lambda \leq 1$ and $\theta > 0$. Convergence was confirmed by letting the process terminated if θ, λ changes by < 0.001 between iterations. The simulation schemes were presented in Tables 1 – 5 respectively.

Table 1. MLE simulation scheme for different parameters values.

	$\theta = 1.5;\ \lambda = 0.5$				$\theta = 0.1;\ \lambda = 1.0$				$\theta = 0.01;\ \lambda = -1$			
N	**MSE θ**	**Bias θ**	**MSE λ**	**Bias λ**	**MSE θ**	**Bias θ**	**MSE λ**	**Bias λ**	**MSE θ**	**Bias θ**	**MSE λ**	**Bias λ**
20	0.07848	0.10701	0.10232	0.14344	0.00087	0.02303	0.28151	0.45426	0.00000	0.00028	0.19620	0.16600
40	0.06064	0.06929	0.10065	0.09997	0.00058	0.01643	0.21537	0.34144	0.00000	0.00003	0.09090	0.06560
60	0.05039	0.05795	0.10003	0.07886	0.00042	0.01133	0.15589	0.24365	0.00000	0.00003	0.05450	0.04610
80	0.05018	0.05607	0.09630	0.07663	0.00035	0.00957	0.13484	0.20895	0.00000	0.00002	0.02830	0.02210
100	0.04767	0.05214	0.09419	0.06758	0.00027	0.00758	0.10888	0.16551	0.00000	0.00002	0.01860	0.01450
500	0.0095	0.0104	0.0188	0.0135	0.00001	0.0015	0.0218	0.0331	0.00000	0.00000	0.0037	0.0029
900	0.0053	0.0058	0.0105	0.0075	0.000003	0.00084	0.0121	0.0184	0.00000	0.00000	0.0021	0.0016

Table 2. MOM simulation scheme for different parameters values.

	$\theta = 1.5;\ \lambda = 0.5$				$\theta = 0.1;\ \lambda = 1.0$				$\theta = 0.01;\ \lambda = -1$			
N	**MSE θ**	**Bias θ**	**MSE λ**	**Bias λ**	**MSE θ**	**Bias θ**	**MSE λ**	**Bias λ**	**MSE θ**	**Bias θ**	**MSE λ**	**Bias λ**
20	0.27880	0.38928	0.57010	-0.46036	0.00029	0.00530	0.04374	-0.01806	0.00000	0.00062	0.20695	-0.07053
40	0.15680	0.17946	0.33528	-0.35502	0.00012	0.00040	0.04318	-0.05330	0.00000	-0.00022	0.10478	0.02245
60	0.29091	0.42654	0.52331	-0.55748	0.00010	0.00105	0.02362	0.04720	0.00000	0.00067	0.08571	-0.16289
80	0.08058	0.12125	0.18037	-0.19611	0.00023	0.00590	0.05925	-0.10650	0.00000	-0.00017	0.08281	0.09288
100	0.07898	0.20037	0.25169	-0.37676	0.00005	-0.00243	0.00821	0.02317	0.00000	0.00003	0.02954	-0.06562
500	0.01576	0.04007	0.05034	-0.07535	0.00001	-0.00049	0.00164	0.00463	0.00000	0.00001	0.00591	-0.01312
900	0.00876	0.02226	0.02797	-0.04186	0.00001	-0.00027	0.00091	0.00257	0.00000	0.00000	0.00328	-0.00729

From Tables 1–5, we noticed that the bias decreases when the sample size increases which indicates unbiasedness. Consistency is an important property for estimators; by collecting a significant number of observations, we aim to collect a lot of information about any unknown parameter θ, thus we search for an estimator

Table 3. LSE simulation scheme for different parameters values.

	$\theta = 1.5;\ \lambda = 0.5$				$\theta = 0.1;\ \lambda = 1.0$				$\theta = 0.01;\ \lambda = -1$			
N	**MSE θ**	**Bias θ**	**MSE λ**	**Bias λ**	**MSE θ**	**Bias θ**	**MSE λ**	**Bias λ**	**MSE θ**	**Bias θ**	**MSE λ**	**Bias λ**
20	0.14740	0.02423	0.23555	0.22155	0.00104	0.01449	0.34995	-0.12033	0.00000	-0.00001	0.35672	0.15345
40	0.05060	-0.07847	0.14259	0.12334	0.00046	0.00890	0.28933	-0.22890	0.00000	-0.00060	0.20873	0.17419
60	0.07670	-0.08244	0.20925	0.25380	0.00075	0.00963	0.32449	-0.11277	0.00000	0.00005	0.07218	0.02337
80	0.04910	-0.01522	0.08087	0.10705	0.00055	0.01180	0.23079	-0.22412	0.00000	-0.00007	0.05036	0.07263
100	0.04607	-0.08072	0.09741	0.10399	0.00028	0.00283	0.14860	-0.09714	0.00000	-0.00030	0.04766	0.04753
500	0.00921	-0.01614	0.01948	0.02080	0.00006	0.00057	0.02972	-0.01943	0.00000	-0.00006	0.00953	0.00951
900	0.00512	-0.00897	0.01082	0.01156	0.00003	0.00031	0.01651	-0.01079	0.00000	-0.00003	0.00530	0.00528

Table 4. WLS simulation scheme for different parameters values.

	$\theta = 1.5;\ \lambda = 0.5$				$\theta = 0.1;\ \lambda = 1.0$				$\theta = 0.01;\ \lambda = -1$			
N	**MSE θ**	**Bias θ**	**MSE λ**	**Bias λ**	**MSE θ**	**Bias θ**	**MSE λ**	**Bias λ**	**MSE θ**	**Bias θ**	**MSE λ**	**Bias λ**
20	0.13491	0.02217	0.17564	0.19490	0.00106	0.01636	0.34245	-0.19436	0.00000	0.00008	0.22766	0.11678
40	0.04811	-0.08220	0.11868	0.11411	0.00045	0.00922	0.25954	-0.24716	0.00000	-0.00049	0.12496	0.13107
60	0.07084	-0.08382	0.16401	0.24621	0.00062	0.00872	0.24221	-0.10873	0.00000	0.00015	0.04300	0.00536
80	0.04452	-0.02230	0.06796	0.10383	0.00046	0.01051	0.17454	-0.20537	0.00000	-0.00004	0.02399	0.05727
100	0.04760	-0.09759	0.09093	0.12933	0.00026	0.00180	0.11165	-0.07204	0.00000	-0.00023	0.02495	0.02539
500	0.00952	-0.01952	0.01819	0.02587	0.00005	0.00036	0.02233	-0.01441	0.00000	-0.00005	0.00499	0.00508
900	0.00529	-0.01084	0.01011	0.01437	0.00003	0.00020	0.01241	-0.00801	0.00000	-0.00003	0.00277	0.00282

Table 5. CVM simulation scheme for different parameters values.

	$\theta = 1.5;\ \lambda = 0.5$				$\theta = 0.1;\ \lambda = 1.0$				$\theta = 0.01;\ \lambda = -1$			
N	**MSE θ**	**Bias θ**	**MSE λ**	**Bias λ**	**MSE θ**	**Bias θ**	**MSE λ**	**Bias λ**	**MSE θ**	**Bias θ**	**MSE λ**	**Bias λ**
20	0.15412	-0.05372	0.41048	0.39376	0.00106	0.01636	0.34245	-0.19436	0.00000	0.00008	0.22766	0.11678
40	0.06589	-0.12312	0.20187	0.22110	0.00045	0.00922	0.25954	-0.24716	0.00000	-0.00049	0.12496	0.13107
60	0.08796	-0.10010	0.27156	0.30194	0.00062	0.00872	0.24221	-0.10873	0.00000	0.00015	0.04300	0.00536
80	0.05472	-0.03677	0.10823	0.15186	0.00046	0.01051	0.17454	-0.20537	0.00000	-0.00004	0.02399	0.05727
100	0.05257	-0.09149	0.12630	0.13128	0.00026	0.00180	0.11165	-0.07204	0.00000	-0.00023	0.02495	0.02539
500	0.01051	-0.01830	0.02526	0.02626	0.00005	0.00036	0.02233	-0.01441	0.00000	-0.00005	0.00499	0.00508
900	0.00584	-0.01017	0.01403	0.01459	0.00003	0.00020	0.01241	-0.00801	0.00000	-0.00003	0.00277	0.00282

with a minimal mean square error (MSE). It is clear from Tables 1–5 that as the number of observations increases the MSE descends to zero.

6. Applications

To examine the flexibility of the proposed model, two datasets are presented. The proposed model has been compared with Monsef distribution, Rayleigh distribution and Pareto distribution. These distributions are used to fit the data, and the parameter estimates are calculated. Some goodness-of-fit tests were used as Kolmogorov-Smirnov (KS), Anderson Darling (AD), Cramer Von-Mises (CVM) and Watson test (WT). Some discrimination criteria were also calculated such as Akaike Information Criterion (AIC), Bayesian information criterion (BIC), Corrected Akaike Information Criterion (AICC), Hannan-Quinn Information Criterion (HQIC) and Consistent Akaike Information Criterion (CAIC).

6.1. Data 1

The first data provided illustrates the the number of days 72 guinea pigs survived after being injected with different doses of tubercle bacilli (Bjerkedal, 1960).

2, 24, 34, 44, 54, 57, 60, 61, 65, 70, 76, 84, 95, 109, 129, 146, 233, 297, 15, 32, 38, 48, 54, 58, 60, 62, 67, 72, 76, 85, 96, 110, 131, 175, 258, 341, 22, 32, 38, 52, 55, 58, 60, 63, 68, 73, 81, 87, 98, 121, 143, 175, 258, 341, 24, 33, 43, 53, 56, 59, 60, 65, 70, 75, 83, 91, 99, 127, 146, 211, 263, 376.

The data was modeled using the QRTMD, Monsef distribution, DUS-Powered Inverse Rayleigh Distribution (DUS-PIR), Power Generalized DUS Transformation of Inverse Kumaraswamy Distribution (PGDUS-IK), DUS Topp–Leone Exponential Distribution (DUS-TLE) and Exponential distribution. The parameter estimates, the goodness-of-fit tests and the information criteria were summarized in Tables 6 and 7.

Table 6. Goodness-of-fit tests for Data 1.

Model	**MLEs**	**KS**	**p-value**	**AD**	**CVM**	**WT**
QRTMD	$\widehat{\theta} = 0.026$ $\widehat{\lambda} = 0.515$	0.149	0.080	2.316	0.370	0.261
Monsef	$\widehat{\theta} = 0.030$	0.181	0.018	3.395	0.599	0.357
DUS-PIR	$\widehat{\theta} = 0.390$ $\widehat{\lambda} = 0.101$	0.322	0.000	11.285	2.272	1.688
PGDUS-IK	$\widehat{\theta} = 0.310$ $\widehat{\lambda} = 0.900$	0.509	0.000	25.079	5.461	3.649
DUS-TLE	$\widehat{\theta} = 0.010$ $\widehat{\lambda} = 0.151$	0.770	0.000	109.264	16.843	3.858
Exponential	$\widehat{\theta} = 0.010$ $\widehat{\lambda} = 0.900$	0.210	0.004	4.159	0.770	0.633

Table 7. Information criteria for Data 1.

Model	**-Loglik**	**AIC**	**BIC**	**AICC**	**HQIC**	**CAIC**
QRTMD	397.259	798.519	803.072	798.693	800.332	798.693
Monsef	399.775	801.550	803.826	801.607	802.456	801.607
DUS-PIR	427.999	859.998	864.551	860.172	861.811	860.172
PGDUS-IK	483.658	971.316	975.869	971.489	973.128	971.489
DUS-TLE	510.286	1024.573	1029.126	1024.746	1026.385	1024.746
Exponential	402.689	809.378	813.931	809.552	811.191	809.552

6.2. Data 2

The following data, from Nichols and Padgett (2006), represents the behaviour of the tensile strength about 100 observations of carbon fibres.

3.7, 3.11, 4.42, 3.28, 3.75, 2.96, 3.39, 3.31, 3.15, 2.81, 1.41, 2.76, 3.19, 1.59, 2.17, 3.51, 1.84, 1.61, 1.57, 1.89, 2.74, 3.27, 2.41, 3.09, 2.43, 2.53, 2.81, 3.31, 2.35, 2.77, 2.68, 4.91, 1.57, 2., 1.17, 2.17, 0.39, 2.79, 1.08, 2.88, 2.73, 2.87, 3.19, 1.87, 2.95, 2.67, 4.2, 2.85, 2.55, 2.17, 2.97, 3.68, 0.81, 1.22, 5.08, 1.69, 3.68, 4.7, 2.03, 2.82, 2.5, 1.47, 3.22, 3.15, 2.97, 1.61, 2.05, 3.6, 3.11, 1.69, 4.9, 3.39, 3.22, 2.55, 3.56, 2.38, 1.92, 0.98, 1.59, 1.73, 1.71, 1.18, 4.38, 0.85, 1.8, 2.12, 3.65

The data was fitted using the same distributions in Data 1. The parameter estimates, the goodness-of-fit tests and the information criteria were summarized in Tables 8 and 9.

The flexibility of the proposed model was examined using two real-world datasets. Standard goodness-of-fit tests and information criteria were employed for the evaluation. While information criteria penalize model

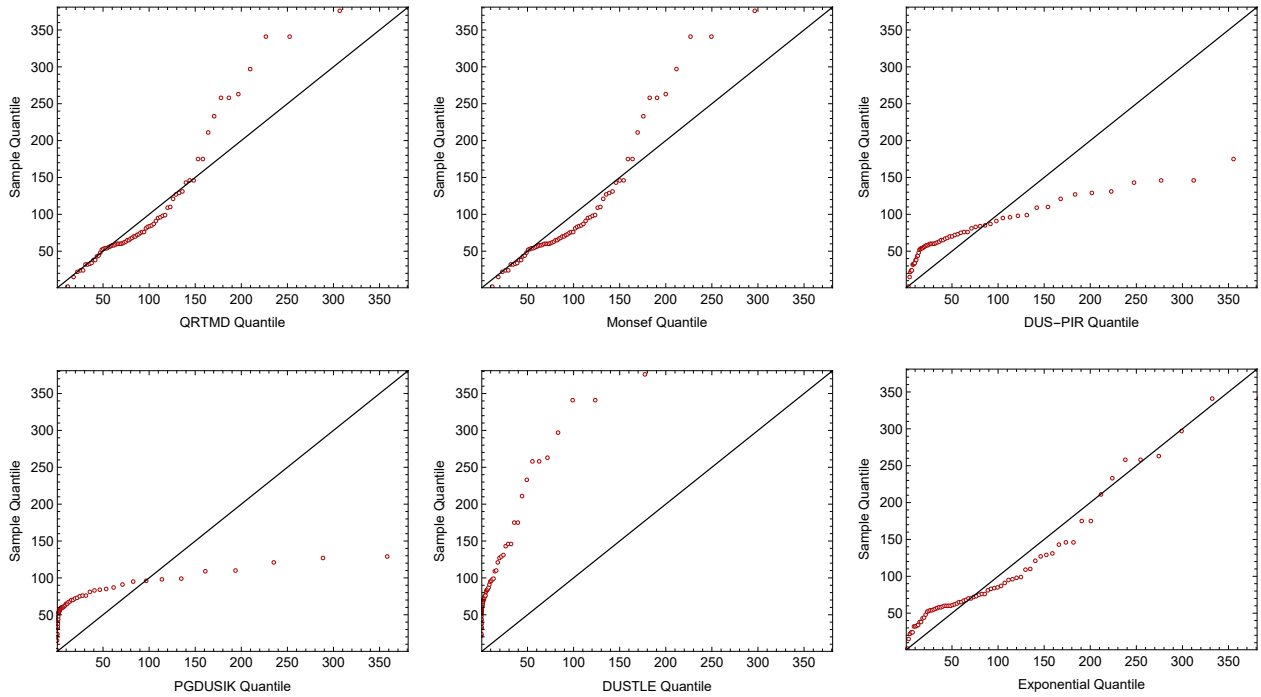

Figure 4. The Q-Q plot of the fitted distributions for the first data

Table 8. Goodness-of-fit tests for Data 2.

Model	**MLEs**	**KS**	**p-value**	**AD**	**CVM**	**WT**
QRTMD	$\widehat{\theta} = 1.196$ $\widehat{\lambda} = -0.900$	0.199	0.00198	6.236	1.225	0.579
Monsef	$\widehat{\theta} = 0.8665$	0.2320	0.00017	8.0779	1.4325	1.1376
DUS-PIR	$\widehat{\theta} = 0.997$ $\widehat{\lambda} = 0.270$	0.249	0.00004	6.559	1.296	0.588
PGDUS-IK	$\widehat{\theta} = 0.892$ $\widehat{\lambda} = 0.900$	0.366	0.00000	20.042	4.009	3.451
DUS-TLE	$\widehat{\theta} = 0.251$ $\widehat{\lambda} = 0.901$	0.342	0.00000	15.798	3.233	1.799
Exponential	$\widehat{\theta} = 0.550$ $\widehat{\lambda} = 0.219$	0.409	0.00000	23.922	5.169	1.890

complexity, the primary goal here was to compare overall fit rather than prioritize parsimony. As shown in Tables 6–9, the QRTMD yields the smallest values across all information criteria and goodness-of-fit statistics against its competitors. This superior quantitative performance is supported visually by the Q-Q plots for the six fitted models (Figures 4 and 5). Based on this combined evidence, the QRTMD is selected as the most appropriate model for both datasets compared to the alternative distributions.

Table 9. Information criteria for Data 2.

Model	-Loglik	AIC	BIC	AICC	HQIC	CAIC
QRTMD	135.342	274.684	279.616	274.827	276.670	274.827
Monsef	148.76	299.52	301.99	299.57	300.50	299.57
DUS-PIR	158.041	320.082	325.014	320.225	322.068	320.225
PGDUS-IK	208.340	420.680	425.612	420.823	422.666	420.823
DUS-TLE	164.775	333.549	338.481	333.692	335.535	333.692
Exponential	167.346	338.691	343.623	338.834	340.677	338.834

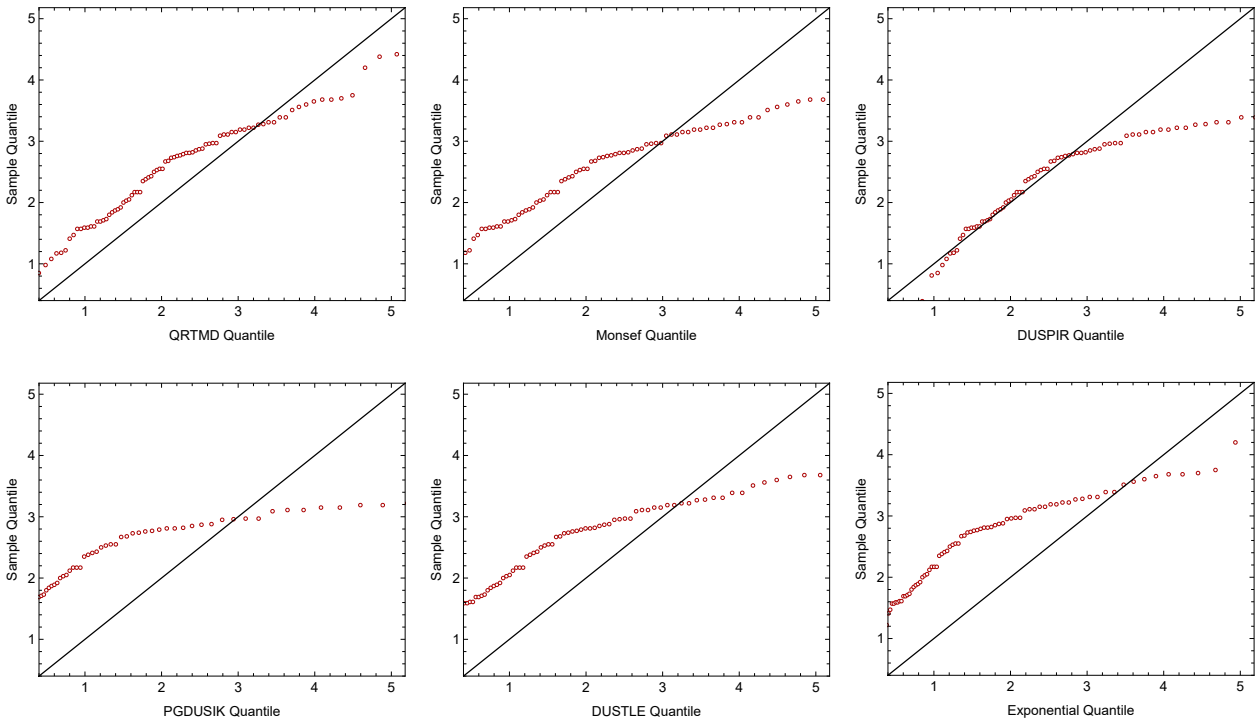

Figure 5. The Q-Q plot of the fitted distributions for the second data

7. Conclusion

This study introduced a new distribution, the Quadratic Rank Transmuted Monsef Distribution (QRTMD), generated by applying the Quadratic Rank Transmutation map to the Monsef baseline distribution. We derived its key statistical properties and reliability measures and evaluated its parameter estimation via a simulation study, which confirmed that the estimates converge to the true parameter values as the sample size increases. The model's practical flexibility was demonstrated through its superior performance over competing distributions in modeling two real-world datasets. Finally, constructing higher-order rank transmutation maps is identified as a promising direction for future research.

Appendix

- The 3^{rd} and 4^{th} moments about the means can be derived as:

$$\begin{aligned}\mu_3 = &-\frac{1}{32\theta^3\left(2+\theta(2+\theta)\right)^6}\Bigg(-64\left(2+\theta(2+\theta)\right)^3\Big(24+\theta\big(72+\theta(108+\theta(100\\&+\theta(54+\theta(12+\theta)))))\big)\Big)+12\left(2+\theta(2+\theta)\right)^2\Big(20+\theta\big(80+\theta(160+\theta(224\\&+\theta(269+2\theta(134+\theta(70+\theta(14+\theta)))))\big)\Big)\lambda\\&+6\left(2+\theta(2+\theta)\right)\left(15+2\theta\left(15+\theta\left(15+\theta(6+\theta)\right)\right)\right)\Big(30+\theta\big(90+\theta(135\\&+2\theta(66+\theta(39+\theta(10+\theta))))\big)\Big)\lambda^2\\&+\left(15+2\theta\left(15+\theta\left(15+\theta(6+\theta)\right)\right)\right)^3\lambda^3\Bigg)\end{aligned} \tag{A.1}$$

$$\begin{aligned}\mu_4 = &\frac{1}{256\theta^4(2+\theta(2+\theta))^8}3\Bigg(-\lambda^4(15+2\theta(15+\theta(15+\theta(6+\theta))))^4\\&-8\lambda^3(2+\theta(2+\theta))(15+2\theta(15+\theta(15+\theta(6+\theta))))^2\Big(30+\theta\big(90+\theta(135\\&+2\theta(66+\theta(39+\theta(10+\theta))))\big)\Big)-64\lambda^2(2+\theta(2+\theta))^2(15+2\theta(15+\theta(15\\&+\theta(6+\theta))))\Big(100+\theta\big(400+\theta(800+\theta(964+\theta(778+\theta(437\\&+\theta(157+2\theta(14+\theta)))))\big)\Big)+256(2+\theta(2+\theta))^4\Big(240+\theta\big(960+\theta(1920\\&+\theta(2304+\theta(1816+\theta(944+\theta(304+3\theta(16+\theta)))))\big)\Big)-64\lambda(2+\theta(2+\theta))^3\\&\Big(600+\theta\big(3000+\theta(7500+\theta(12048+\theta(13550+\theta(10974+\theta(6519\\&+2\theta(1396+\theta(386+3\theta(18+\theta)))))\big)\Big)\Bigg)\end{aligned} \tag{A.2}$$

- β_1 and β_2 are given as follows:

$$\begin{aligned}\beta_1 = &-\left[4\Big(-64A(\theta)^3B(\theta)+12A(\theta)^2C(\theta)\,\lambda+6A(\theta)D(\theta)E(\theta)\,\lambda^2+D(\theta)^3\,\lambda^3\Big)^2\right]\\&\div\Big(-16A(\theta)^2G(\theta)+4A(\theta)E(\theta)\,\lambda+D(\theta)^2\,\lambda^2\Big)^3\end{aligned}$$

where

$$\begin{aligned}A(\theta) &= \theta(\theta+2)+2\\B(\theta) &= 24+\theta(72+\theta(108+\theta(100+\theta(54+\theta(12+\theta)))))\\C(\theta) &= 20+\theta(80+\theta(160+\theta(224+\theta(269+2\theta(134+\theta(70+\theta(14+\theta))))))))\\D(\theta) &= 15+2\theta(15+\theta(15+\theta(6+\theta)))\\E(\theta) &= 30+\theta(90+\theta(135+2\theta(66+\theta(39+\theta(10+\theta)))))\\G(\theta) &= 12+\theta(2+\theta)(12+\theta(6+\theta))\end{aligned} \tag{A.3}$$

and

$$\begin{aligned}\beta_2 =& \frac{3}{\left(-16A(\theta)^2G(\theta)+4A(\theta)E(\theta)\lambda+D(\theta)^2\lambda^2\right)^2}\times\\ &\Big(256\,A(\theta)^4\,J(\theta)-64\,A(\theta)^3\,K(\theta)\,\lambda-D(\theta)^4\,\lambda^4\\ &\quad-64\,A(\theta)^2\,D(\theta)\,L(\theta)\,\lambda^2-8\,A(\theta)\,D(\theta)^2\,E(\theta)\,\lambda^3\Big)\end{aligned}$$

where:

$$\begin{aligned}A(\theta) &= \theta(\theta+2)+2\\ J(\theta) &= 240+\theta(960+\theta(1920+\theta(2304+\theta(1816+\theta(944+\theta(304+3\theta(16+\theta)))))))\\ K(\theta) &= 600+\theta(3000+\theta(7500+\theta(12048+\theta(13550+\theta(10974+\theta(6519\\ &\quad+2\theta(1396+\theta(386+3\theta(18+\theta)))))))))\\ L(\theta) &= 100+\theta(400+\theta(800+\theta(964+\theta(778+\theta(437+\theta(157+2\theta(14+\theta))))))\\ D(\theta) &= 15+2\theta(15+\theta(15+\theta(6+\theta)))\\ E(\theta) &= 30+\theta(90+\theta(135+2\theta(66+\theta(39+\theta(10+\theta)))))\\ G(\theta) &= 12+\theta(2+\theta)(12+\theta(6+\theta))\end{aligned} \tag{A.4}$$

- The MGF and the CHF of X, denoted by $M_X(t)$ and $\phi_x(t)$ are derived as follows:

$$\begin{aligned}M_X(t) =& -\frac{\theta^3}{(t-2\theta)^5(t-\theta)^3A(\theta)^2}\times\\ &\Bigg[(t-2\theta)^5A(\theta)\big(2+t^2-2t(1+\theta)+A(\theta)\big)\\ &\quad+t\lambda\Big(t^6A(\theta)-2t^5\Big(2+\theta\big(14+\theta(13+5\theta)\big)\Big)\\ &\qquad+8\theta^4D(\theta)-8t\theta^3\Big(30+\theta\big(75+2\theta(45+\theta(21+4\theta))\big)\Big)\\ &\qquad+4t^2\theta^2\Big(40+\theta\big(140+\theta(215+2\theta(59+13\theta))\big)\Big)\\ &\qquad-4t^3\theta\Big(10+\theta\big(60+\theta(130+\theta(85+22\theta))\big)\Big)\\ &\qquad+t^4\Big(4+\theta\big(48+\theta(168+\theta(132+41\theta))\big)\Big)\Big)\Bigg]\end{aligned}$$

where

$$\begin{aligned}A(\theta) &= \theta(\theta+2)+2\\ D(\theta) &= 15+2\theta(15+\theta(15+\theta(6+\theta)))\end{aligned} \tag{A.5}$$

$$\begin{aligned}\phi_x(t) =& \frac{\theta^3}{(t+i\theta)^3(t+2i\theta)^5 A(\theta)^2} \times \\ & \Bigg[32\theta^5 A(\theta)^2 + it^7 A(\theta)(1+\lambda) \\ & - 8t^2\theta^3\Big(2A(\theta)\big(10+\theta(20+17\theta)\big) + K(\theta)\lambda\Big) \\ & + 4it^3\theta^2\Big(10A(\theta)\big(2+\theta(6+7\theta)\big) + L(\theta)\lambda\Big) \\ & + 2t^4\theta\Big(5A(\theta)\big(2+\theta(10+17\theta)\big) + 2M(\theta)\lambda\Big) \\ & - 2t^6\Big(2(1+\lambda) + 14\theta(1+\lambda) + 13\theta^2(1+\lambda) + \theta^3(6+5\lambda)\Big) \\ & - 8it\theta^4\Big(5(8+3\lambda) + 2\theta\big(48+15\lambda+\theta(56+15\lambda+\theta(32+6\lambda+\theta(9+\lambda)))\big)\Big) \\ & - it^5\Big(4(1+\lambda) + \theta\Big(48(1+\lambda) + \theta\big(168(1+\lambda) + \theta(144+132\lambda+\theta(61+41\lambda))\big)\Big)\Big)\Bigg]\end{aligned}$$

where

$$\begin{aligned} A(\theta) &= \theta(\theta+2)+2 \\ K(\theta) &= 30+\theta\big(75+2\theta(45+\theta(21+4\theta))\big) \\ L(\theta) &= 40+\theta\big(140+\theta(215+2\theta(59+13\theta))\big) \\ M(\theta) &= 10+\theta\big(60+\theta(130+\theta(85+22\theta))\big) \end{aligned} \tag{A.6}$$

Ethics approval and Consent to participate

Not applicable.

Consent for publication

Not applicable.

Availability of data and materials

The authors confirm that the data supporting the findings of this study are available within the article.

Competing interests

The authors declare that they have no Conflict of interest.

Authors' contributions

MME conceived of the presented idea. All authors developed theoretical formalism, performed the analytic calculations and performed the numerical simulations. Both MME and TA contributed to the final version of the manuscript. HH contributed to the analysis of the results and to the writing of the manuscript.

Acknowledgements

The authors wish to express their gratitude to the referees for their valuable comments and suggestions, which significantly enhanced the quality of this paper.

REFERENCES

1. Abate, J., Choudhury, G.L., Lucantoni, D.M. and Whitt, W. (1995). Asymptotic analysis of tail probabilities based on the computation of moments. The Annals of Applied Probability. 5(4), 983–1007.
2. Abd El-Monsef M (2020). Erlang Mixture Distribution with Application on COVID-19 Cases in Egypt, International Journal of Biomathematics. 14:03.
3. Abd El-Monsef, M.M.E. and Alshrani, M. (2020). The weighted Monsef distribution. African Journal of Mathematics and Computer Science Research. 13(2), 74-84.
4. Abd El-Monsef, M.M.E., Sohsah, N.M. and Hassanein, W.A. (2021). Unit Monsef Distribution with Regression Model. Asian Journal of Probability and Statistics. 15(4) 330-340.
5. Al-Faris, R. Q., & Khan, S. (2008). Sine square distribution: a new statistical model based on the sine function. Journal of Applied Probability and Statistics, 3(1), 163-173.
6. Alzaatreh A, Lee C, Famoye F. (2013). A new method for generating families of continuous distributions. Metron. 71, 63-79.
7. Ameeq, M., Naz, S., Tahir, M., Muneeb Hassan, M., Jamal, F., Fatima, L., and Shahzadi, R. (2024). A new Marshall-Olkin Lomax distribution with application using failure and insurance data. Statistics, 58(2), 450–472.
8. Aryal, G.R. and Tsokos, C.P. (2009). On the transmuted extreme value distribution with application. Nonlinear Analysis: Theory, Methods and Applications. 71 (12), 1401–1407.
9. Bjerkedal, T. (1960). Acquisition of Resistance in Guinea Pigs Infected with Different Doses of Virulent Tubercle Bacilli. The American Journal of Epidemiology. 72, 130-148.
10. Gauthami, P., & Chacko, V. M. (2024). Power Generalized DUS Transformation of Inverse Kumaraswamy Distribution and Stress-Strength Analysis. Society of Statistics, Computer and Applications, 18(1), 323-338.
11. Gupta, R.C., Gupta, R.D. and Gupta, P.L. (1998). Modeling failure time data by Lehman alternatives. Communication in Statistics-Theory and Methods. 27 (4), 887-904.
12. Imran, M., Bakouch, H. S., Tahir, M. H., Ameeq, M., Jamal, F., and Mendy, J. T. (2023). A new Bell-exponential model: Properties and applications. Cogent Engineering, 10(2).
13. Khan, M. I., & Mustafa, A. (2023). Powered Inverse Rayleigh Distribution Using DUS Transformation. International Journal of Analysis and Applications, 21(6), 61-75.
14. Kumar D, Singh U, Singh SK. (2015). A method of proposing new distribution and its application to bladder cancer patients' data. Journal of Statistics Applications & Probability Letters. 2(3), 235–245.
15. Megha, C. M., Divya, P. R., & Sajesh, T. A. (2025). Neutrosophic DUS Exponential Distribution. Neutrosophic Sets and Systems, 79(1), 110–116.
16. Mohammed, S. O., Hassan, W. O., & Yahaya, A. (2024). DUS Topp-Leone-G Family of Distributions: Baseline Extension, Properties, Estimation, Simulation and Useful Applications. Mathematics, 12(11), 973.
17. Nichols, M.D. and Padgett, W.J. (2006). A Bootstrap Control Chart for Weibull Percentiles, Quality and Reliability Engineering International. 22, 141–151.
18. Shaw, W.T. and Buckley, I.R. (2007). The alchemy of probability distributions: beyond Gram-Charlier expansions and a skew kurtotic-normal distribution from a rank transmutation map. arXiv:0901.0434.
19. Thomas, B., & Chacko, V. M. (2023). Power Generalized DUS Transformation in Weibull and Lomax Distributions. CyberLeninka.
20. Unnikrishnan, J. M., Chacko, V. M., & Thomas, B. (2023). Generalized Dinesh-Umesh-Sanjay generalized exponential distribution with application to engineering data. AIP Advances, 13(11), 115228.